Facile Fabrication of Diblock Methoxy Poly(ethylene glycol)-poly(tetramethylene carbonate) and Its Self-Assembled Micelles as Drug Carriers

Jun Feng,* Wei Su, Hua-fen Wang, Fu-wei Huang, Xian-zheng Zhang, and Ren-xi Zhuo

Key Laboratory of Biomedical Polymers (The Ministry of Education), Department of Chemistry, Wuhan University, Wuhan 430072, People's Republic of China

ABSTRACT AB type diblock methoxy poly(ethylene glycol)-*b*-poly(tetramethylene carbonate) (mPEG-PTeMC) copolymers were designed for the first time and used as carriers for the sustained release of the hydrophobic drug ibuprofen. In this paper, we developed a facile ring-opening polymerization (ROP) method to prepare mPEG-PTeMC copolymers under the catalysis of Novozym-435 lipase. Attractively, the polymerization has been successfully performed at 30 °C, close to room temperature. The data show that the copolymer compositions agree well with the feed ratio of TeMC to mPEG, indicating the controllable feature of the polymerization. The copolymer structures were characterized by ^{1}H NMR, IR, SEC, and DSC measurements. mPEG-PTeMC exhibits no apparent in vitro cytotoxicity toward human embryonic kidney transformed 293T cells. Those amphiphilic copolymers can readily self-assemble into nanosized micelles (about 150 nm) in aqueous solution. Their critical micelle concentrations are in the range of $(1.6-9.3) \times 10^{-7}$ mol/L, determined by fluorescence spectroscopy. The micelles present high stability in PBS solution, with no obvious change in micelle diameters over 5 days. Ibuprofen can be loaded effectively in mPEG-PTeMC micelles, and its sustained release behavior is observed. Transmission electron microscopy shows that the well-dispersed spherical micelles are around 25 nm in diameter, while the diameter is 30 nm after loading ibuprofen. The release rate increases when the chain length of the PTeMC block decreases. These properties show that the micelles self-assembled from mPEG-PTeMC copolymers would have great potential as carriers for the effective encapsulation as well as sustained release of hydrophobic drugs.

KEYWORDS: cytotoxicity • drug release • micelle • nanoparticle • polycarbonate • polyethylene oxide

INTRODUCTION

Clinical applications of many therapeutic drugs are hindered due to their low water solubility, high toxicity, and susceptibility to inactivation in the physiological environment. To overcome those obstacles, considerable efforts have been devoted to the construction of long-circulating drug delivery systems based on amphiphilic block copolymers (1). These copolymers, consisting of both hydrophilic and hydrophobic segments, can readily self-assemble into nanosized micelles in aqueous medium, resulting in a core−shell structure (2−4). The formed hydrophobic "core" is able to serve as an effective reservoir for toxic and poorly water-soluble drugs and therapeutic DNA as well as protein drugs (5−7). This procedure improves the efficiency of the therapeutic treatment by preserving the drug in its active form and by limiting its possible toxic effects. Furthermore, the nanometer size of drug-loaded micelles contributes much to the intravascular delivery, crossing biological barriers and passive target effect to tumor tissues. Poly(ethylene glycol), known as PEG, is a nontoxic, highly hydrated polymer and has been approved by the FDA for internal use (8−10). It frequently acts as the hydrophilic segments to build the "shell" of the micelles from amphiphilic block copolymers (11). The flexible PEG "shell" with high mobility can endow drug-loaded micelles with special biological functions such as more prolonged circulation half-time in blood and reduced uptake rate by the reticuloendothelial system (RES) as well as the absence of antigenicity and immunogenicity (12). PEG-based amphiphilic copolymers and their micelles represent a major advance for the development of continuous and controlled drug delivery systems.

At present, aliphatic polyesters, including polycaprolactone, polylactide, and poly(DL-lactic acid-co-glycolic acid) (PLGA), appear to hold a leading position in building the hydrophobic core of polymeric micelles for drug delivery system design (13−16). Research in this area is greatly encouraged, due to their biodegradability, biocompatibility, and acceptable stability at processing temperatures. However, previous work on the encapsulation of some drugs such as proteins and plasmid DNA into PLGA microspheres led to the conclusion that these drugs may suffer an inactivation process in the course of polymer degradation. This process was mainly caused by the acidic microenvironment created by the accumulation of degraded polyester oligomers inside the microspheres (17−20). Aliphatic polycarbonates, represented by poly(trimethylene carbonate) (PTMC), is one

* To whom correspondence should be addressed. Tel: + 86 27 6875 4509. Fax: + 86 27 6875 4509. E-mail: fengjun@whu.edu.cn.

Received for review July 2, 2009 and accepted November 9, 2009

DOI: 10.1021/am900452c

important type of biodegradable polymer with excellent mechanical properties and biocompatibility (21, 22). Some of the PTMC copolymers have been commercialized and used for clinical application (23). Aliphatic polycarbonates can degrade in vivo by a surface erosion process without the formation of acidic degradation compounds (24−26). This is especially attractive in controlled drug delivery applications. Our group and other researchers have described the synthesis and self-assembly behavior of di- or triblock copolymer systems based on PEG and PTMC with a linear or star-shaped structure (22, 27−31). The reported copolymers have been demonstrated to be effective carriers for the sustained release of hydrophobic drugs such as anticancer drugs.

In recent years, increasing attention has been paid to research on poly(tetramethylene carbonate) (PTeMC) (32, 33). One main factor is in consideration of its marked difference in properties compared to PTMC as well as the much cheaper price of butylene glycol used for PTeMC preparation, which makes PTeMC more attractive for industrial production and medical applications. Relative to amorphous PTMC, PTeMC readily crystallizes and is more hydrophobic. In general, the stronger hydrophobicity of the core-forming polymers can improve the efficiency of physical drug entrapment driven by the hydrophobic interactions between drug and core-forming polymers. Also, it contributes to the tendency of the polymer chain association for micelle formation, resulting in greater thermodynamic stability to withstand micelle dissociation and the consequent premature release of loaded drugs after entry into the bloodstream (34−36). The crystalline or semicrystalline nature of polymers may also contribute to micelle stability and confer greater drug retention properties due to the reduced fluidity of the polymer core (37). Moreover, PTeMC has a lower degradation rate than PTMC and many other biopolyesters (24). This would be advantageous in biomedical or environmental applications where relatively higher stability is desired.

With these facts in mind, the present paper aimed at developing a drug delivery system based on block copolymers consisting of PEG and PTeMC for the first time. Ibuprofen is a poorly water-soluble anti-inflammatory drug, and it is desirable to obtain a better micellar solubilization of this drug in clinical applications. Therefore, it was employed as the model for exploring the potential of nanosized PEG-PTeMC micelles for the delivery of hydrophobic drugs. The ideal drug delivery system should be biocompatible, and it is also expected to be obtainable through simple synthesis. Herein the fabrication of PEG-PTeMC is designed through facile ring-opening polymerization (ROP) of TeMC using PEG as the initiator (Scheme 1). As is known, stannous octoate ($SnOCt_2$) is an excellent catalyst for the ROP of cyclocarbonates as well as lactones and has been widely applied for the manufacture of biomedical polyesters and polycarbonates (38). However, recent studies have shown that $SnOCt_2$ has a toxic effect on cells and can be accumulated in the body (39, 40). On the other hand, biosynthetic pathways such as enzymatic ROP have attracted great attention as a new trend

Scheme 1. Lipase-Catalyzed Synthesis of mPEG-PTeMC Copolymers

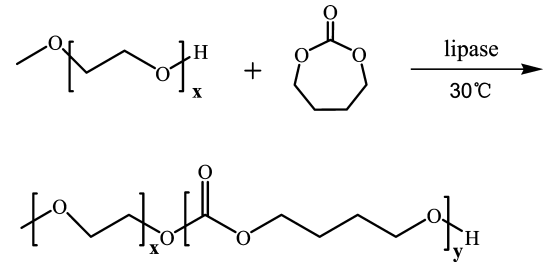

of biomaterial synthesis due to their nontoxicity and mild reaction requirements (41). Thus, immobilized lipase Novozym-435 was adopted in this work to catalyze the ROP of TeMC at 30 °C. To our knowledge, the successful achievement of enzymatic ring-opening polymerization at such a low temperature has not yet been reported.

EXPERIMENTAL SECTION

Materials. Tetramethylene carbonate (TeMC) was synthesized according to the method in ref 42. Methyl PEG (mPEG, $M_n = 2000$) was purchased from Sigma and dried under vacuum at 40 °C for 48 h before use. Lipase acrylic resin from *Candida antarctica* (Novozym-435) was used as received from Sigma. Molecular sieve-4A was dehydrated at 400 °C for 6 h before use. Toluene was received from Shanghai Chemical Reagent Co. and distilled over Na/K alloys. All other solvents and reagents were used as received without further treatments.

Preparation of mPEG-PTeMC Diblock Copolymers. A tube equipped with a magnetic stir bar was charged with a certain amount of mPEG, 100 mg of TeMC, 0.6 mL of fresh toluene, and molecular sieves. After the mixture was stirred for 2 h, 5.5 mg of Novozym-435 was added. The tube was closed with a glass stopper and immersed in an oil bath thermstated at 30 °C. After 48 h, the polymerization was quenched by introducing 3 mL of dichloromethane. The insoluble Novozym-435 was filtered away. After concentration, the solution was dropped into a large amount of mixed solvent (1/3 methanol/ether, v/v) to isolate the polymer product. mPEG-PTeMC block copolymers with different chemical compositions were prepared by changing the molar ratio of TeMC monomer to mPEG initiator. The unit ratio of TeMC to EG (PEG unit) and the average molecular weight of those copolymers were obtained by comparing the peak intensities of the methylene proton in TeMC at δ 4.1 ppm ($-CH_2OC(O)O-$) (A_{PTeMC}) to that of PEG units at δ 3.6 ppm ($-OCH_2$) (A_{PEG}) from the ^{1}H NMR spectra:

$$\text{unit ratio} = A_{PTeMC}/A_{PEG}$$

$$M_n(\text{copolymer}) = M_n(\text{PEG}) + M_n(\text{PTeMC})$$

$$= 2000 + \text{fw(TeMC)} \times 45 \times \text{unit ratio}$$

where M_n(PEG) and M_n(PTeMC) correspond to the M_n values of the mPEG and PTeMC blocks, respectively. fw(TeMC) is the formula weight of the TeMC unit, and the value of 45 was the number of repeated units of mPEG used ($M_n = 2000$).

^{1}H NMR and FT-IR Characterization. ^{1}H NMR spectra were recorded on a Mercury VX-300 spectrometer at 300 Hz using $CDCl_3$ or D_2O as the solvent. IR spectra were recorded on a Perkin-Elmer-2 spectrometer. Samples were film-cast in chloroform onto sodium chloride plates.

SEC Measurements. Size exclusion chromatography (SEC) was carried out on a Waters HPLC system equipped with a Model 2690D separation module, a Module 2410 differential

refractive index detector, and a Shodex K803 column. THF was used as the eluent at a flow rate of 1.0 mL/min. The sample concentration and injection volume were 0.3% (w/v) and 20 μL, respectively.

DSC Measurements. Differential scanning calorimetry (DSC) measurements were carried on a Perkin-Elmer DSC 7 thermal analyzer. The copolymers and their micellar particles obtained by lyophilization were subjected to DSC measurements in an identical manner with a heating rate of 10 °C/min and a cooling rate of 5 °C/min, respectively.

Micelle Formation. The micelles of mPEG-PTeMC copolymers were produced by a dialysis method. Briefly, the copolymers were dissolved in THF at an initial concentration of 200 mg/L and subjected to dialysis against 1800 mL of distilled water for 24 h using a dialysis tube (molecular weight cutoff 3500). The distilled water was replaced every 6 h to remove THF.

Determination of Critical Micelle Concentration (CMC). Fluorescence spectra were recorded on a LS55 luminescence spectrometer (Perkin-Elmer). Pyrene was used as a hydrophobic fluorescent probe to determine the CMC. Aliquots of pyrene solutions (1×10^{-3} M in acetone, 6 μL) were added to containers, and the acetone was allowed to evaporate at room temperature. One milliliter portions of aqueous copolymer solutions at different concentrations were then added to the containers containing the pyrene residue. The solutions were kept at room temperature for 24 h to reach the solubilization equilibrium of pyrene in the aqueous phase. Excitation was carried out at 340 nm, and emission spectra were recorded in the range 350−500 nm. Excitation and emission bandwidths were both 5 nm. From the pyrene emission spectra, the fluorescence intensity ratio of the third and first vibronic bands (I_3/I_1) was plotted against the logarithm of the copolymer concentrations. A CMC value was determined from the intersection of the tangent to the curve at the inflection with the horizontal tangent through the points at low concentration.

TEM Measurement. Transmission electron microscopy (TEM) was carried out with a JEM-100CX II instrument at an acceleration voltage of 100 keV. In brief, a drop of the micelle suspension (containing micelles with no drug and micelles with drug loading), produced just as above, was placed on a copper grid with Formvar film and stained with a 0.2% (w/v) solution of phosphotungstic acid before measurement.

Micelle Size Distribution and Micelle Stability. The mean particle size and size distribution of self-assembled micelles in the aqueous phase were determined using dynamic light scattering (DLS) techniques with a Nano-ZS ZEN3600 instrument. Each sample was diluted to a concentration of 30 mg/L with distilled water and passed through a 0.45 μm pore size filter before measurement. To investigate the micelle stability at a specific diameter, the solutions were directly subjected to DLS measurement after a predetermined interval.

Drug Loading and in Vitro Drug Release. The experiments were carried out according to the method of ref 43. The micelles with drug loading were prepared as follows: mPEG-PTeMC copolymer (6 mg) and ibuprofen (3 mg) were dissolved in 9 mL of THF. The solution was put into a dialysis tube (molecular weight cutoff 3500) and subjected to dialysis against 1800 mL of distilled water for 24 h, and the distilled water was replaced every 6 h to remove THF and unloaded drug.

After drug loading, the dialysis tube was directly immersed into 10 mL of PBS (pH 7.4, $I = 0.1$) for in vitro release test at 37.4 °C. The ibuprofen was allowed to diffuse freely from the inside of the dialysis tube to the outside PBS medium after release from the micelles. At the setting interval, the solution was withdrawn and the same volume of refresh PBS was added. The amount of ibuprofen in PBS released from micelles was determined on the basis of the UV absorbance intensity at 264 nm, using a standard calibration curve experimentally obtained. The mass of drug loaded in micelles contained the total cumulative mass of drug released and the drug unreleased which still remained in the micelles. To determine the unreleased drug, the micelle solution after drug release was lyophilized and dissolved in 10 mL of DMF and the value obtained by UV absorbance at 272 nm. We define the drug release efficiency (DRE) and the entrapment efficiency (EE) as

$$\text{DRE (wt \%)} = (\text{mass of drug released}/\text{mass of drug loaded in micelles}) \times 100\%$$

$$\text{EE (wt \%)} = (\text{mass of drug loaded in micelles}/\text{mass of drug fed initially}) \times 100\%$$

In Vitro Cytotoxicity Test. For each well in a 96-well plate, 100 μL of Human embryonic kidney transformed 293T cells in DMEM, with a concentration of 6×10^4 cells/mL, was added. The number of 293T cells in each well was 6×10^3. After incubation for 24 h in an incubator (37 °C, 5% CO_2), the culture medium was changed to 200 μL of DMEM containing mPEG-PTeMC$_2$ at particular concentrations and the mixture was further incubated for 48 h. Then, 20 μL of MTT solution (5 mg/mL) was added to every well. After incubation for 4 h, the solution was removed, 200 μL of DMSO was added, and the mixture was shaken at room temperature. The optical density (OD) was measured at 570 nm with a Microplate Reader Model 550 (Bio-Rad). The viable rate was calculated by the equation

$$\text{viable rate} = (\text{OD}_{\text{treated}}/\text{OD}_{\text{control}}) \times 100\%$$

where $\text{OD}_{\text{control}}$ was obtained in the absence of mPEG-PTeMC$_2$ and $\text{OD}_{\text{treated}}$ was obtained in the presence of mPEG-PTeMC$_2$.

RESULTS AND DISCUSSION

Synthesis and Structure of mPEG-PTeMC Copolymers. PEG-coated triblock copolymers lead to the formation of PEG coils on the surface with two anchoring points to the core. For the same PEG chain length, the maximum coating thus obtained would be half as thick as that obtained when diblock polymers are used. As a result, the PEG coating on triblock nanospheres would be less effective than the one on diblock particles, in order to prevent opsonization and increase blood circulation times (17). Hence in this paper, diblock PEG-PTeMC was designed and used rather than triblock PTeMC-PEG-PTeMC.

The hydroxyl groups of methyl-PEG-OH (mPEG-OH) were used as the initiation sites for the ring-opening polymerization of TeMC with a catalyst of Novozym-435 to produce the diblock copolymers (Scheme 1). As the control, no polymerization was observed in the absence of Novozym-435, which demonstrates that the enzyme catalysis is an indispensable factor for the polymerization. It is interesting to point out that all the polymerizations could be carried out at 30 °C. To our knowledge, Novozym-435 usually shows high catalytic activity toward the polymerization of lactones and TMC at higher temperatures in the range of 60−100 °C (41). The successful achievement of the polymerization at such a low temperature is possibly due to the high ring strain of TeMC.

Four copolymer products were obtained and denoted mPEG-PTeMC$_1$, mPEG-PTeMC$_2$, mPEG-PTeMC$_3$, and mPEG-PTeMC$_4$, respectively, as shown in Table 1. These copolymers have different PTeMC lengths, while the lengths of the hydrophilic mPEG ($M_n = 2000$) blocks were identical, thus allowing us to investigate the effect of copolymer composi-

Table 1. Reaction Conditions and Molecular Composition of the Copolymers

block copolymer[a]	feed weight ratio[b] [TeMC]/[mPEG]	composition ratio[c] [PTeMC]/[mPEG]	M_n[d]	M_w/M_n[e]
mPEG-PTeMC$_1$	50:50	39:61	5100	1.82
mPEG-PTeMC$_2$	25:75	24:76	8500	2.01
mPEG-PTeMC$_3$	17:83	16:84	12500	1.83
mPEG-PTeMC$_4$	9:91	10:90	21000	1.71

[a] All the samples were prepared by using mPEG-OH with M_n = 2000. [b] Weight ratios of TeMC to mPEG in feed. [c] Weight ratios of PTeMC block to mPEG block from mPEG-PTeMC copolymers based on ^{1}H NMR analysis. [d] Determined by NMR analysis. [e] Estimated by SEC.

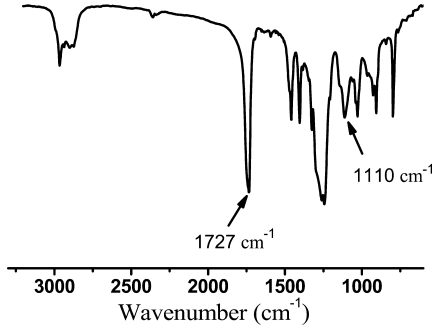

FIGURE 1. IR spectrum of mPEG-PTeMC$_2$ copolymer.

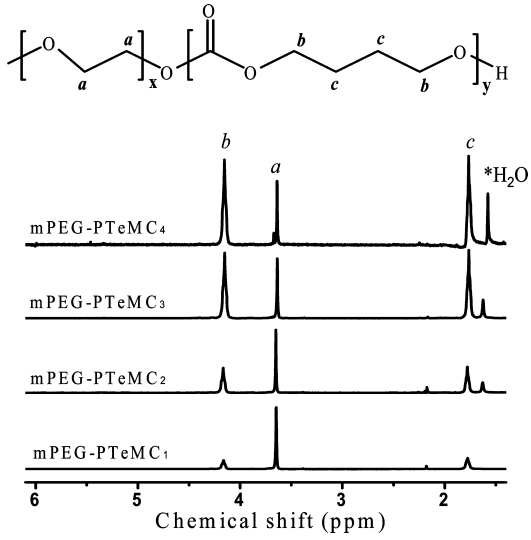

FIGURE 2. ^{1}H NMR spectra of mPEG-PTeMC copolymers.

tions on the micelle properties. As exhibited in the FT-IR spectrum of mPEG-PTeMC (Figure 1), all of the characteristic signals for PTeMC and PEG segments appear. The carbonyl stretch for the PTeMC block occurs at 1727 cm^{-1}, and the ether stretch exists at 1110 cm^{-1} for the PEG block. ^{1}H NMR spectra of mPEG-PTeMC in $CDCl_3$ (Figure 2) show the presence of characteristic resonances of mPEG-PTeMC block copolymers. Figure 3 includes the SEC traces for the resulting four copolymers together with mPEG (M_n = 2000). Only a unimodal symmetric peak exists in the SEC curves for all the four copolymers, which suggests that the products are not a mixture of homopolymers of PTeMC and PEG. Furthermore, the peak shifts toward lower retention times (higher molecular weights) with an increasing feed ratio of

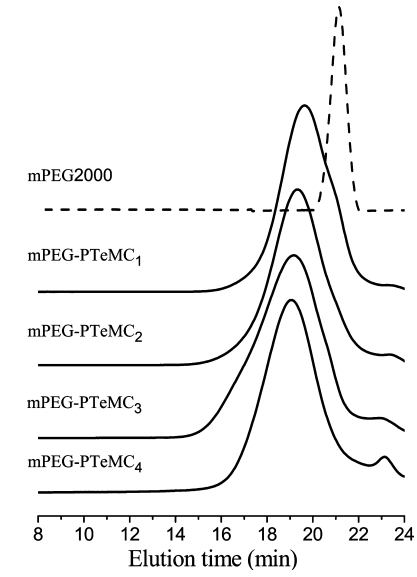

FIGURE 3. SEC profiles of four mPEG-PTeMC copolymers and mPEG (M_n = 2000).

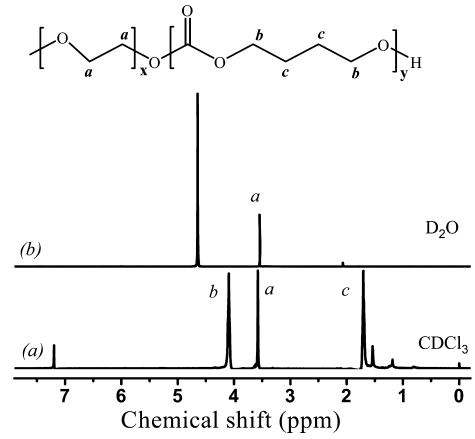

FIGURE 4. ^{1}H NMR spectra of mPEG-PTeMC$_3$ in $CDCl_3$ (a) and D_2O (b).

TeMC to mPEG, indicating an increasing trend in copolymer molecular weight. Taken together, these data strongly prove the successful synthesis of the copolymers.

The accurate number-average molecular weights and block compositions of mPEG-PTeMC copolymers can be determined from the ratio between integrals of peaks for PTeMC and PEG segments, which are summarized in Table 1. The resulting data indicate that copolymer compositions agree well with the feed ratios. The polymerizations have controllable features.

Structure of mPEG-PTeMC Micelles. The amphiphilic nature of the block copolymers, consisting of hydrophilic mPEG and hydrophobic PTeMC blocks, provides an opportunity to form micelles in water. The characteristics of the block copolymer micelles in an aqueous phase were investigated by NMR analysis. ^{1}H NMR spectra of the mPEG-PTeMC$_3$ in $CDCl_3$ and D_2O, as a representative example, are presented in Figure 4. It has been shown that the characteristic resonance originating from PTeMC is almost lost when using D_2O as the NMR solvent (Figure 4b). The micelle shells consisting of PEG blocks are well solvated in D_2O and

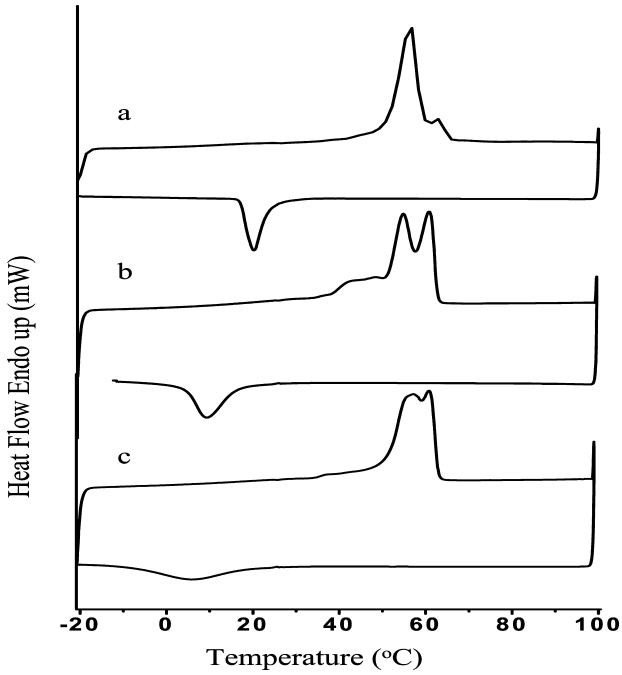

FIGURE 5. DSC heating and cooling curves of the copolymers mPEG-PTeMC$_1$ (a), mPEG-PTeMC$_2$ (b), and mPEG-PTeMC$_3$ (c). Conditions: heating rate, 10 °C/min; cooling rate, 5 °C/min.

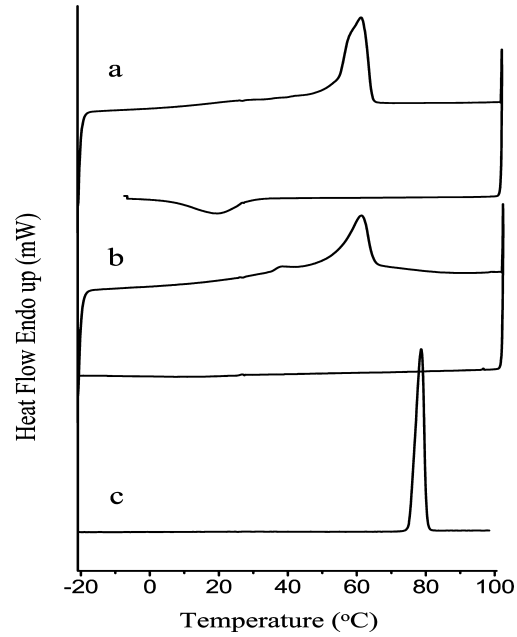

FIGURE 6. DSC curves of the micelle particles (mPEG-PTeMC$_2$(micelle)) (a), ibuprofen-loaded micelle particles (mPEG-PTeMC$_2$(drug)) (b), and free ibuprofen (c).

therefore show clear ^{1}H NMR signals. The complete loss of a characteristic PTeMC resonance in the case of D_2O medium is due to suppressed molecular motion of the aggregated PTeMC chains surrounded by the hydrophilic PEG block. Thus, ^{1}H NMR analysis reveals a core−shell micellar structure of mPEG-PTeMC copolymers with a completely isolated hydrophobic inner core of PTeMC and a hydrophilic outer shell of long PEG extended in an aqueous phase.

Thermal Properties of mPEG-PTeMC Diblock Copolymers and Their Micelle Particles. Thermal properties of mPEG-PTeMC diblock copolymers with different PTeMC contents were investigated by DSC measurements in an identical manner. The heating rate was 10 °C/min, and the following cooling course was fixed at a rate of 5 °C/min. Homopolymers of PEG (M_n = 2000) and PTeMC (M_n = 10 000) were semicrystalline; their melting transition temperatures (T_m) were 59 and 62 °C, respectively. The T_m value of PTeMC was reported to depend little on the molecular weight (44). Although the homopolymers of both mPEG and PTeMC have comparable melting temperatures, DSC curves of mPEG-PTeMC copolymers distinctly exhibit bimodal endothermic peaks (Figure 5). This demonstrates that phase separation takes place in the block copolymers to form PTeMC and PEG domains, respectively. As the chain length of PTeMC (of the mPEG-PTeMC diblock copolymer) increases, the peak intensity at higher temperature increases in the heating curve. Therefore, the higher temperature melting peaks can be attributed to the PTeMC domain and the lower ones can be attributed to the PEG domain, respectively. It can be found that melting transition temperatures of PTeMC and PEG segments in the copolymers are both lower than those of their homopolymers, indicating that crystallization of PTeMC blocks and PEG blocks influences each other. As can be seen from Figure 5, only one exothermic peak appears in the cooling curve, which correresponds to the crystallizing temperature (T_c) of PEG. The absence of a T_c value for PTeMC could find an explanation in previous reports that PTeMC crystallizes very slowly, and at least 1 h of annealing is required before a significant degree of crystallinity is detectable in the second DSC heating scan for high-molecular-weight PTeMC (M_w = 50 000) homopolymer (44). Moreover, for the given PEG block length (M_n = 2000), the crystallizing transition peak of the PEG domain is at lower temperature and is broader in the case of longer PTeMC length. It can be explained that the presence of a PTeMC block would restrict the crystallization of mPEG segments. Also, this restriction would be more pronounced in the case of a higher content of PTeMC block. This phenomenon is in agreement with previous DSC studies performed on mPEG-PTMC diblock and PCL/PEG/PCL triblock copolymers (21, 45).

For comparison, DSC measurement was also applied to free mPEG-PTeMC$_2$ copolymer without micellization treatment (mPEG-PTeMC(free)), its micelle particles (mPEG-PTeMC(micelle)), and ibuprofen-loaded micelle particles (mPEG-PTeMC(drug)) (Figure 6). Interestingly, when mPEG-PTeMC$_2$ is in the state of micelle particles, its DSC heating curve exhibits one broad peak rather than the bimodal peak which is found for mPEG-PTeMC(free). Generally speaking, the phase separation between hydrophilic and hydrophobic domains in the micelle particles is supposed to be much stronger compared to that before micellization. Thus, for mPEG-PTeMC(micelle), the restriction of PEG crystallization resulting from the coexistence of PTeMC appears to be relatively lower. The hypothesis is demonstrated by the increased Tc of mPEG-PTeMC(micelle) relative to that of mPEG-PTeMC(free) (Figure 6). In that sense, the melting transition peak of PEG would also be increased, and conse-

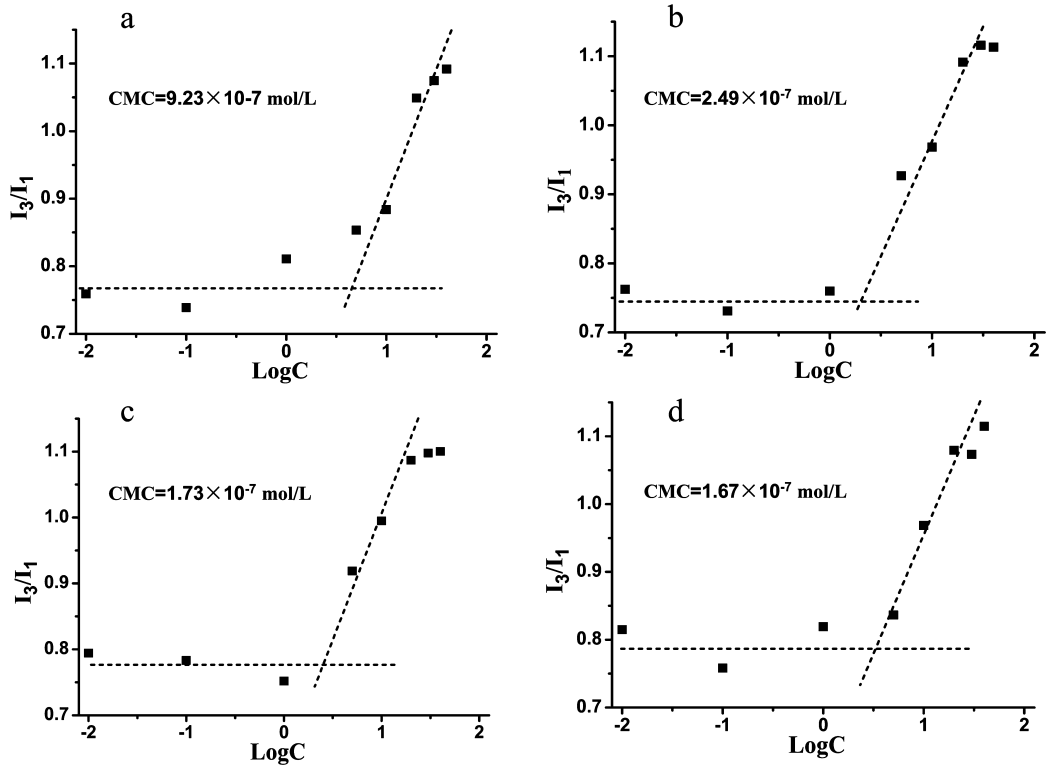

FIGURE 7. Plot of the fluorescence intensity of I_3/I_1 in the emission spectra versus the logarithm of the concentration of mPEG-PTeMC$_1$ (a), mPEG-PTeMC$_2$ (b), mPEG-PTeMC$_3$ (c), and mPEG-PTeMC$_4$ (d).

quently, overlapping melting peaks of PEG and PTeMC were observed for mPEG-PTeMC(micelle). In the DSC curve of mPEG-PTeMC(drug), there is no ibuprofen melting transition peak to be found, indicating that ibuprofen is molecularly dispersed in the polymer matrix. Nevertheless, the T_c peak of PEG is also not observed. This suggests that ibuprofen is not only possibly embedded in the PTeMC core but also partly adsorbed into the shell of micelles, which restrict the crystallization of PEG block. One possible explanation for the ibuprofen adsorptions is that during the drug-loading course followed by lyophilization, a small amount of soluble ibuprofen is retained in the hydrophilic PEG shell domains.

CMC of mPEG-PTeMC Micelles. The formation of the micelles from mPEG-PTeMC copolymers in aqueous medium was also verified by a fluorescence probe technique. Pyrene was used here as a hydrophobic fluorescent probe for its high sensitivity to the local polarity of the pyrene environment. The intensity ratio I_3/I_1 was monitored as a function of each mPEG-PTeMC concentration (Figure 7).

A negligible change in intensity ratio (I_3/I_1) is detected at a low concentration range, but at a certain concentration the intensity ratio I_3/I_1 exhibits a substantial increase, corresponding to the onset of micelle formation as well as the simultaneous incorporation of pyrene into the hydrophobic core region of the micelles. Therefore, the critical micellar concentration (CMC) was determined from the crossover point at the low concentration range in Figure 7. The CMC values for mPEG-PTeMC$_1$, mPEG-PTeMC$_2$, mPEG-PTeMC$_3$, and mPEG-PTeMC$_4$ are 9.23×10^{-7}, 2.49×10^{-7}, 1.73×10^{-7}, and 1.67×10^{-7} mol/L, respectively. Obviously, the CMC values of mPEG-PTeMCs are dependent on the block composition, showing a tendency to decrease as the length of the PTeMC chain increases. Furthermore, the low CMC values provide evidence for an apparent stability and allow their use in very dilute aqueous milieu such as body fluids.

Hydrophile−lipophile balance (HLB) value is usually utilized to evaluate the hydrophobic/hydrophilic ability of amphiphilic compounds. To understand the micellization behavior, the HLB value was calculated on the basis of the composition of mPEG-PTeMC copolymers according to the equation

$$\mathrm{HLB} = \frac{W_H}{W_H + W_L} \times 20$$

Here, W_H and W_L correspond to the weight fractions of the hydrophilic PEG segment and lipophilic PTeMC segment, respectively. HLB values of mPEG-PTeMC$_1$, mPEG-PTeMC$_2$, mPEG-PTeMC$_3$, and mPEG-PTeMC$_4$ are 8.28, 4.95, 2.49, and 1.99, respectively. The HLB values decrease as the length of the PTeMC chains increases, suggesting increasing lipophilic or hydrophobic ability. Thus, the tendency for variation of CMC values is more probably due to the stronger hydrophobic interactions in the "core" domain with an increase in chain length of PTeMC.

Morphology of the Micelles. The morphology and size distribution of polymer micelles were investigated by transmission electron microscopy (TEM) and dynamic light scattering (DLS). It can be seen from TEM pictures (Figure 8) that the self-assembled micelles are well dispersed as individual nanoparticles with an average diameter of about 25 nm. The micelles of mPEG-PTeMC block copolymers are regularly spherical without secondary aggregation observed

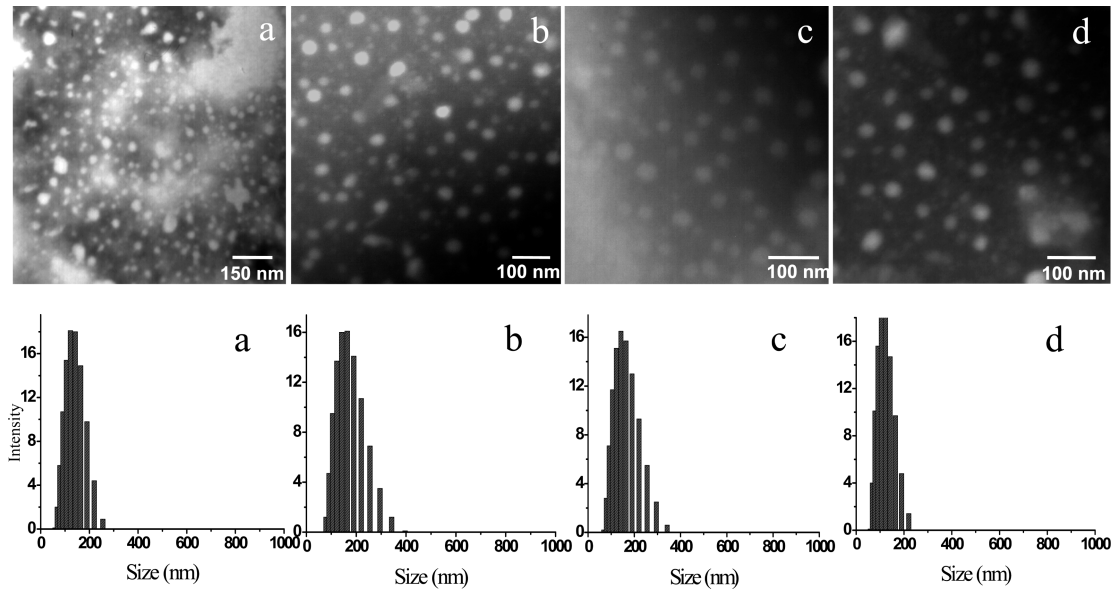

FIGURE 8. TEM pictures of the micelles from mPEG-PTeMC$_1$ (a), mPEG-PTeMC$_2$ (b), mPEG-PTeMC$_3$ (c), and mPEG-PTeMC$_4$ (d) and their corresponding size distributions detected by DLS in distilled water.

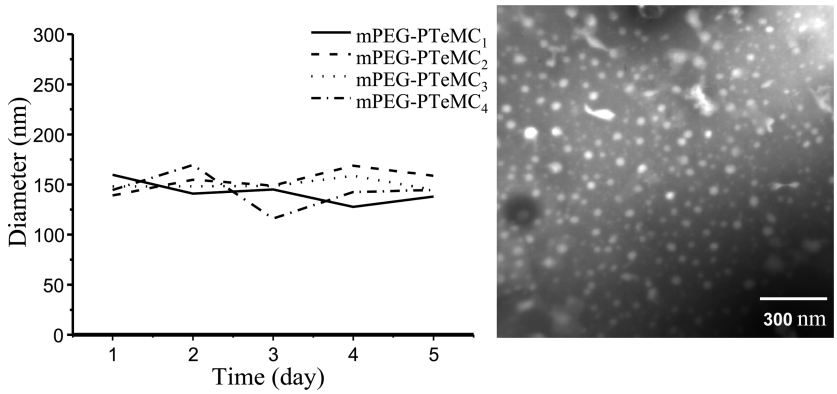

FIGURE 9. Variation of micelle diameters as a function of incubation time and TEM picture of redispersed mPEG-PTeMC$_3$ micelle after storage for 1 month.

between individual micelles. In comparison, the hydrodynamic diameters of micelles from DLS are in the range 120−180 nm. The size distribution values of micelles were moderate in the range 0.182−0.235 determined by DLS. The difference in micelle size measured by DLS and TEM should be attributed to the fact that the former is the hydrodynamic diameter of micelles in water, whereas the latter reveals the morphology size of the micelles in the solid state. Similar differences in size as a result of different measuring techniques were also reported elsewhere (46, 47). The DLS and TEM experiments indicate that mPEG-PTeMC micelles are more likely to adopt a simple core−shell structure, rather than a multicore structure which is formed by the association of individual micelles. Meanwhile, no distinct relationship could be observed between the micelle size and copolymer composition in this work. The four copolymers prepared are almost similar in micelle diameters. This may be possibly due to the highly compact core resulting from the strong hydrophobic interaction of the PTeMC chains.

Stability of the Micelles. The stability of the micelles was evaluated by DLS and TEM measurements. For all four mPEG-PTeMC copolymers, the average sizes of the micelles in aqueous medium determined by DLS vary little after standing for 5 days (Figure 9). At all times the size distribution values remain below 0.24, confirming the stability of the micelles. This conclusion seems of great significance for intravenous drug delivery, since it implies the stable maintenance of the micelles in the bloodstream. The nanosphere powders of mPEG-PTeMC$_3$ were recovered by the lyophilization after dialysis method. After 1 month, the powders were found to readily redisperse well in aqueous solutions. TEM (Figure 9) confirms that the shape and size of the consequently formed mPEG-PTeMC$_3$ micelles has no obvious change. Nanosphere powders thus show good shelf storage properties.

In Vitro Cytotoxicity Test. Biocompatibility is a great concern for the family of biomaterials. In this study, we performed a preliminary evaluation of the in vitro cytotoxicity of the obtained copolymers by the MTT assay. The representative result of mPEG-PTeMC$_2$ is shown in Figure 10, and it reveals that mPEG-PTeMC$_2$ exhibits very low cytotoxicity toward 293T cells.

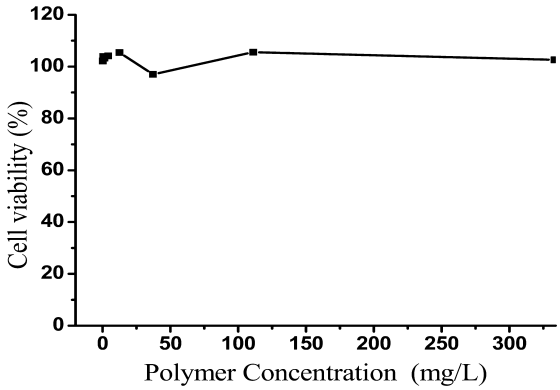

FIGURE 10. In vitro cytotoxicity of mPEG-PTeMC2 with different concentrations.

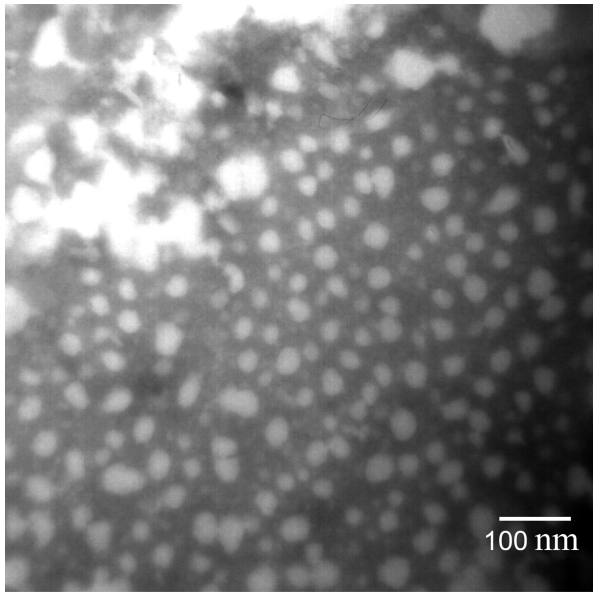

FIGURE 11. TEM picture of the micelle from ibuprofen-loaded mPEG-PTeMC$_3$ copolymer.

Drug Loading. It is known that a hydrophobic drug can be physically loaded and stabilized in the hydrophobic micellar inner core by hydrophobic interactions. Herein we chose ibuprofen as a model drug and prepared the corresponding drug-loaded micelles by the dialysis technique. About 2.2 mg of the drug was loaded in 6 mg of polymer micelles with a mean entrapment efficiency (EE) of around 73% when the initial feed drug is 3 mg, which indicates that hydrophobic ibuprofen can be effectively loaded into the micelles. The morphology of drug-loaded polymeric nanoparticles was observed by TEM, and a representative result for mPEG-PTeMC$_3$ is shown in Figure 11. The image shows that nanoparticles are still regularly spherical in shape with a diameter of about 30 nm.

In Vitro Drug Release. In vitro release of ibuprofen was carried out in PBS (0.1 M, pH 7.4) at 37.4 °C. The obtained data (Figure 12) show a continuous release over 32 h. After the burst release in the first 5 h, entrapped ibuprofen was released at a slow rate for the next 27 h. The burst release behavior is possibly due to fast diffusion of the ibuprofen adsorbed in PEG domains. On the other hand, a trend is found that the drug release rate is enhanced as the

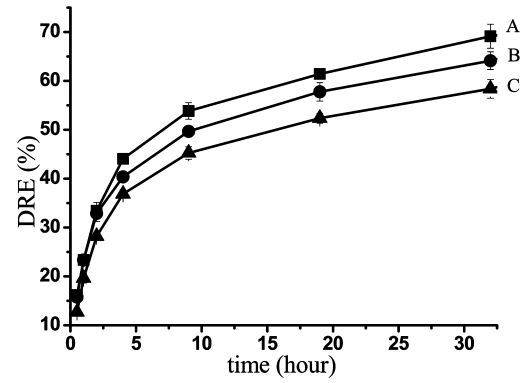

FIGURE 12. Drug release profiles for copolymers mPEG-PTeMC$_1$ (C), mPEG-PTeMC$_3$ (B), and mPEG-PTeMC$_4$ (A).

PTeMC length decreases. This suggests that the drug release rate can be tailed in a controlled manner by modulating the composition of copolymers.

As can be seen from all the resulting data, in aqueous medium, PEG-PTeMC can readily self-assemble into nanosized micelles, with a functional PEG "shell" and a PTeMC "core" to load hydrophobic drugs. Taking into account the high drug loading of the micelles and the sustained drug release behavior over time, there is a possibility that with further study PEG-PTeMC may be desirable delivery vehicles for most hydrophobic drugs. Furthermore, the nanometer size and high stability of the micelles make the drug-carrier systems suitable for intravenous injection, in addition to oral administration. In comparison with the polyester-based vehicles usually reported, PEG-PTeMC presents a major advance in that it avoids the possible drug inactivation process mainly caused by the acidic microenvironment resulting from degraded polyester oligomers. PEG-PTeMC could also find potential application in the design of a longer circulating drug delivery system, due to the relatively higher stability of PTeMC. In addition, PEG-PTeMC was prepared herein in high yield by enzyme catalysis at a lower temperature of 30 °C. The approach is considered "green" in view of reduced energy use and the nontoxic nature of the biocatalyst. This "green" manufacturing procedure and the low price of butylene glycol used for PTeMC preparation should make PEG-PTeMC more attractive in the future from the standpoint of industrial production.

CONCLUSIONS

A series of diblock methoxy poly(ethylene glycol)-*b*-poly(tetramethylene carbonate) (mPEG-PTeMC) copolymers were prepared under the catalysis of Novozym-435 lipase at 30 °C. The obtained copolymers are composed of hydrophilic mPEG (M_n = 2000) block and hydrophobic PTeMC block with different molecular weights. The resultant data show that copolymer compositions agree well with the feed ratio, indicating the controllable nature of the polymerization. These amphiphilic copolymers can readily self-assemble into nanosized micelles in aqueous solution. The CMC values are in the range (1.6−9.3) × 10^{-7} mol/L determined by fluorescence spectroscopy. The CMC values are found to be dependent on the block composition, showing

a decreasing tendency with the increased length of PTeMC chain. The mean diameters of the micelles are around 150 nm in aqueous solution determined by DLS and around 25 nm in the solid state determined by TEM. The formed micelles exhibit high stability in PBS solution over 5 days, and few aggregations are observed. The in vitro cytotoxicity test suggests that mPEG-PTeMCs exhibit very low cytotoxicity toward human embryonic kidney transformed 293T cells. The micelles can effectively load hydrophobic ibuprofen. DSC measurement indicates that ibuprofen is not only embedded in the micelle core but also possibly adsorbed in the micelle shell domain. The mean diameters of the ibuprofen-loaded micelles are around 30 nm, as determined by TEM. mPEG-PTeMC copolymers show great potential as carriers to develop sustained drug release systems for hydrophobic drugs.

Acknowledgment. This work was financially supported by the National Natural Science Foundation of China (Grant No. 20874075), National Key Basic Research Program of China (Grant Nos. 2005CB623903 and 2009CB930300), and the Ministry of Education of China (Cultivation Fund of Key Scientific and Technical Innovation Project 707043).

REFERENCES AND NOTES

(1) Yoo, H. S.; Park, T. G. *J. Controlled Release* **2001**, *70* (1−2), 63–70.
(2) Kataokaa, K.; Haradaa, A.; Nagasakib, Y. *Adv. Drug Delivery Rev.* **2001**, *47*, 113–131.
(3) Rösler, A.; Vandermeulen, G. W. M.; Klok, H.-A. *Adv. Drug Delivery Rev.* **2001**, *53*, 95–108.
(4) Gaucher, G.; Dufresne, M. H.; Sant, V. P.; Kang, N.; Maysinger, D.; Leroux, J.-C. *J. Controlled Release* **2005**, *109*, 169–188.
(5) Kabanov, A. V.; Batrakova, E. V.; Alakhov, V. Y. *Adv. Drug Delivery Rev.* **2002**, *54*, 759–779.
(6) Gaymalov, Z. Z.; Yang, Z. Z.; Pisarev, V. M.; Alakhov, V. Y.; Kabanov, A. V. *Biomaterials* **2009**, *30*, 1232–1245.
(7) Wei, H.; Zhang, X. Z.; Cheng, C.; Cheng, S. X.; Zhuo, R. X. *Biomaterials* **2007**, *28*, 99–107.
(8) Greenwald, R. B.; Choe, Y. H.; McGuire, J.; Conover, C. D. *Adv. Drug Delivery Rev.* **2003**, *55*, 217–250.
(9) Veronese, F. M.; Pasut, G. *Drug Discovery Today* **2005**, *10*, 1451–1458.
(10) Steinmetz, N. F.; Manchester, M. *Biomacromolecules* **2009**, *10*, 784–792.
(11) Adams, M. L.; Lavasanifar, A.; Kwon, G. S. *J. Pharm. Sci.* **2003**, *92*, 1343–1355.
(12) Gref, R.; Minamitake, Y.; Peracchia, M.; Trubetskoy, V.; Torchilin, V.; Langer, R. *Science* **1994**, *263*, 1600–1603.
(13) Fairley, N.; Hoang, B.; Allen, C. *Biomacromolecules* **2008**, *9*, 2283–2291.
(14) Joung, Y. K.; Lee, J. S.; Park, K. D.; Lee, S. J. *Macromol. Res.* **2008**, *16*, 66–69.
(15) Arimura, H.; Ohya, Y.; Ouchi, T. *Biomacromolecules* **2005**, *6*, 720–725.
(16) Jeong, B.; Bae, Y. H.; Kim, S. W. *Colloids Surf. B* **1999**, *16*, 185–193.
(17) Fu, K.; Pack, D. W.; Klibanov, A. M.; Langer, R. *Pharm. Res.* **2000**, *17*, 100–106.
(18) Tinsley-Bown, A. M.; Fretwell, R.; Dowsett, A. B.; Davis, S. L.; Farrar, G. H. *J. Controlled Release* **2000**, *66*, 229–241.
(19) Walter, E.; Moelling, K.; Pavlovic, J.; Merkle, H. P. *J. Controlled Release* **1999**, *61*, 361–374.
(20) Tobió, M.; Alonso, M. J. *STP Pharma Sci.* **1998**, *8*, 303–310.
(21) Zhang, Z.; Grijpma, D. W.; Feijen, J. *J. Controlled Release* **2006**, *112*, 57–63.
(22) Kim, S. Y.; Kim, H. J.; Lee, K. E.; Han, S. S.; Sohn, Y. S.; Jeong, B. *Macromolecules* **2007**, *40*, 5519–5525.
(23) Watanabe, J.; Kotera, H.; Akashi, M. *Macromolecules* **2007**, *40*, 8731–8736.
(24) Suyama, T.; Tokiwa, Y. *Enz. Microbiol. Tech.* **1997**, *20*, 122–126.
(25) Pranamuda, H.; Chollakup, R.; Tokiwa, Y. *Appl. Environ. Microbiol.* **1999**, *65*, 4220–4222.
(26) Zhang, Z.; Kuijer, R.; Bulstra, S. K.; Grijpma, D. W.; Feijen, J. *Biomaterials* **2006**, *27*, 1741–1748.
(27) Kim, B. S.; Oh, J. M.; Cho, J. S.; Lee, S. H.; Lee, B.; Khang, G.; Lee, H. B.; Kim, M. S. *J. Appl. Polym. Sci.* **2009**, *111*, 1706–1712.
(28) Zhang, H. H.; Huang, Z. Q.; Sun, B. W.; Guo, J. X.; Wang, J. L.; Chen, Y. Q. *J. Polym. Sci., Part A: Polym. Chem.* **2008**, *46*, 8131–8140.
(29) Kim, M. S.; Hyun, H.; Kim, B. S.; Khang, G.; Lee, H. B. *Nano Korea 2006 Symposium*; Ilsan, South Korea, Aug 30−Sep 01, 2006; Ilsan, South Korea, 2006; pp 646−650.
(30) Cho, J. S.; Kim, B. S.; Hyun, H.; Youn, J. Y.; Kim, M. S.; Ko, J. H.; Park, Y. H.; Khang, G.; Lee, H. B. *Polymer* **2008**, *49*, 1777–1782.
(31) Zhang, Y.; Zhuo, R. X. *Biomaterials* **2005**, *26*, 2089–2094.
(32) Matuso, J.; Sanda, F.; Endo, T. *J. Polym. Sci., Part A: Polym. Chem.* **1997**, *35*, 1375–1380.
(33) Feng, J.; Wang, H. F.; Li, S. F.; Zhuo, R. X. *Acta Polym. Sin.* **2008**, 686–690.
(34) Adams, M. L.; Andes, D. R.; Kwon, G. S. *Biomacromolecules* **2003**, *4*, 750–757.
(35) Adams, M. L.; Kwon, G. S. *7th European Symposium on Controlled Drug Delivery*; Noordwijk Aan Zee, The Netherlands, Apr 3–5, 2002; Noordwijk Aan Zee, The Netherlands, 2002; pp 23–32.
(36) Opanasopit, P.; Yokoyama, M.; Watanabe, M.; Kawano, K.; Maitani, Y.; Okano, T. *Pharm. Res.* **2004**, *21*, 2001–2008.
(37) Gaucher, G.; Dufresne, M. H.; Sant, V. P.; Kang, N.; Maysinger, D.; Leroux, J. C. *12th International Symposium on Recent Advances in Drug Delivery Systems*; Salt Lake City, UT, Feb 21−24, 2005; Salt Lake City, UT, 2005; pp 169−188.
(38) Jia, Y. T.; Kim, H. Y.; Gong, J.; Lee, D. R.; Ding, B.; Bhattarai, N. *Polym. Int.* **2004**, *53*, 312–319.
(39) Kricheldorf, H. R. Tubingen, Germany, Aug 23−25, 1999; Tubingen, Germany, 1999; pp 49−54.
(40) Tanzi, M. C.; Verderio, P.; Lampugnani, M. G.; Resnati, M.; Dejana, E.; Sturani, E. *J. Mater. Sci. Mater. Med.* **1994**, *5*, 393–396.
(41) Kobayashi, S.; Uyama, H.; Kimura, S. *Chem. Rev.* **2001**, *101*, 3793–3818.
(42) Takeuchi, D.; Aida, T.; Endo, T. *Macromol. Rapid Commun.* **1999**, *20*, 182–184.
(43) Chang, C.; Wei, H.; Feng, J.; Wang, Z. C.; Wu, X. J.; Wu, D. Q.; Cheng, S. X.; Zhang, X. Z.; Zhuo, R. X. *Macromolecules* **2009**, *42*, 4838–4844.
(44) Kricheldorf, H. R.; Mahler, A. *J. Polym. Sci., Part A: Polym. Chem.* **1996**, *34*, 2399–2406.
(45) Piao, L. H.; Dai, Z. L.; Deng, M. X.; Chen, X. S.; Jing, X. B. *Polymer* **2003**, *44*, 2025–2031.
(46) Chang, C.; Wei, H.; Quan, C. Y.; Li, Y. Y.; Liu, J.; Wang, Z. C.; Cheng, S. X.; Zhang, X. Z.; Zhuo, R. X. *J. Polym. Sci., Part A: Polym. Chem.* **2008**, *46*, 3048–3057.
(47) Giacomelli, C.; Schmidt, V.; Borsali, R. *Macromolecules* **2007**, *40*, 2148–2157.

AM900452C